ELSEVIER

Contents lists available at ScienceDirect

Separation and Purification Technology

journal homepage: www.elsevier.com/locate/seppur





Pressure-driven membrane nutrient preconcentration for down-stream electrochemical struvite recovery

Zahra Anari ^{a,b}, Karla Morrissey ^b, László Kékedy-Nagy ^{b,c}, Raheleh Daneshpour ^{a,b}, Mojtaba Abolhassani ^b, John Moore ^b, Greg Thoma ^b, Lauren Greenlee ^{a,b,*}

- ^a Department of Chemical Engineering, The Pennsylvania State University, University Park, PA 16802, USA
- b Ralph E. Martin Department of Chemical Engineering, University of Arkansas, 3202 Bell Engineering Center, Fayetteville, AR 72701, USA
- ^c Department of Electrical and Computer Engineering, Concordia University, Center of Structural and Functional Genomics, 7141 Sherbrooke St. West, Montreal H4B 1R6, Canada

ARTICLE INFO

Keywords: Nutrient recovery Struvite fertilizer Wastewater treatment Membrane preconcentration Membrane fouling Electrochemical precipitation

ABSTRACT

Nutrient recovery from wastewater is a sustainable solution to combat the harmful release of nutrients to the environment. Here, we investigate nutrient recovery from wastewater by pre-concentration of wastewater nutrients using pressure-driven membranes prior to downstream electrochemical nutrient precipitation. When using electrochemical struvite precipitation, a higher nutrient concentration leads to a higher precipitation efficiency. Therefore, we investigate the performance of commercial nanofiltration (NF) and reverse osmosis (RO) membranes with different polymer chemistry and molecular weight cut-offs (MWCO) and discuss the membrane selection based on design goals and wastewater compositions for maximum nutrient recovery efficiency. Our results indicated that the Alfa membrane, a polyamide thin film composite (PA-TFC) NF membrane with 300 Da MWCO has the highest concentration factor in phosphorus (P) preconcentration among all the membranes studied due to the high flux and removal efficiency. BW30LE (PA-TFC, 100 Da), Synder (PA-TFC, 100-250 Da) and NF90 (PA-TFC, 200-400 Da) achieved a high concentration factor for nitrogen (N) recovery. NF90 and Synder NF membranes are able to achieve a nitrogen concentration factor similar to BW30LE RO membrane at much lower energy consumption. A multistage membrane system design is suggested using the selected membranes for effective nutrient recovery. Life cycle assessment (LCA) was conducted to characterize the environmental impact of the multistage membrane nutrient recovery system. Among the different process configurations of the selected membranes, key trends included: 1) environmental impacts across most categories increased as the number of membranes increased, and 2) as the amount of fertilizer substitute that could be produced in a given configuration increased, total environmental impacts decreased with some exceptions.

1. Introduction

Conventional nitrogen and phosphorus removal from wastewater streams have been primarily focused on nutrient "removal" from the water, but not "recovery". Currently, nitrogen in wastewater is mainly removed through energy-intensive approaches such as biologically mediated nitrification/denitrification, which converts nitrogen compounds into nitrogen gas [1–2]. In addition to energy use and cost, nitrification/denitrification processes convert the energy-dense ammonia molecule to a compound (N_2) that has no value in the food supply system, essentially wasting the energy used to produce ammonia. P recovery using conventional approaches such as simultaneous

precipitation in aeration tanks is also less acceptable due to loss of the phosphate to biosolids waste and the precipitative fouling (scaling) in wastewater treatment plant equipment. Recovery and separation of both ammonia and phosphate in early treatment stages could prevent ammonia loss through biological conversion, as well as unwanted precipitation, which increases equipment fouling and maintenance costs [3], and loss of phosphate.

One target compound for nutrient recovery is struvite (MgNH $_4$ PO $_4$ *6H $_2$ O), a phosphorus mineral with low solubility in neutral pH conditions. The low solubility of struvite causes a slower release of nutrients when used as a fertilizer [4]. This slow-release characteristic results in lower non-point source emissions to water streams as well as

^{*} Corresponding author at: Department of Chemical Engineering, The Pennsylvania State University, University Park, PA 16802, USA. *E-mail address*: greenlee@psu.edu (L. Greenlee).

providing crops with the supply of ammonium, phosphorus, and magnesium, supporting a sustainable agricultural system [5]. Struvite precipitation is a potential nutrient recovery method from municipal and animal wastewater sources. In an electrochemical struvite recovery approach, a magnesium (Mg) electrode provides the required Mg for the precipitation of N and P as struvite [6]. Electrochemical precipitation is advantageous over its competitor, chemical precipitation, with no required chemical addition, inherent pH control, and greater energy efficiency [7]. Previous studies have demonstrated that higher aqueous concentrations of ammonium and phosphate yield greater electrochemical recovery of struvite. Low phosphorus concentration leads to a low precipitation efficiency with a longer operation time [8]. This result suggests preconcentration prior to electrochemical precipitation will enhance N and P recovery. Further, most wastewaters have excess ammonia well above the equimolar requirement for phosphate precipitation in struvite. As a result, high quality liquid fertilizers can also be produced by the concentration of ammonia in wastewater, providing an additional valuable product and simultaneously avoiding resource loss through nitrification/denitrification and nitrogen release to receiving water bodies.

A membrane filtration step may maximize downstream recovery of nutrients and facilitate process optimization of nutrient component separation. Both pressure-driven and osmotically-driven membrane filtration systems are widely investigated in wastewater treatment and demonstrated efficient in resource recovery; however, pressure-driven membrane filtration is advantageous over osmotically-driven membrane systems as the permeate water can be used directly as a product, while in a forward osmosis system, the water is transported through the membrane and mixed with a draw solution that needs a secondary purification process to recover water from the draw solute [9-10]. Nanofiltration (NF) and reverse osmosis (RO) have been shown to have great potential for nutrient rejection and recovery from wastewater [11]. Fine pore sizes of NF/RO membranes can effectively retain dissolved ions by being a physical/electrostatic barrier through size/Donnan exclusion [12-13]. The retention of ions enriches wastewater nutrients, producing retentates that are suitable for down-stream struvite precipitation. In addition, clean permeate water is produced, which can potentially be reused in agricultural/municipal sectors depending on the water reuse regulatory requirements.

Some studies have focused on the purification and recovery of nutrients from NF permeates where the nutrients pass through the larger molecular weight cut-off (MWCO) NF membranes, and the remaining contaminants stay in the retentate. Pronk et al. [14] has investigated the separation of pharmaceuticals from nutrients where nutrients pass through the membrane with the permeate and pharmaceuticals are retained by NF membranes. They found out that among ammonium, phosphate, and urea, urea has a better permeation, and ammonium and phosphate ions are mainly rejected by NF membranes. Niewersch et al. [15] and Blocher et al. [16] have studied P recovery from sewage sludge ash using acid purification and NF membranes to provide a permeate containing purified phosphate.

In this work, we investigated the performance of commercially available NF/RO membranes in wastewater nutrient recovery and presented a multistage membrane system design where the best-performed membranes are used in multiple different configurations for N and P concentration and specific target product recovery (e.g., liquid ammonia fertilizer, struvite precipitate). In addition, we evaluated the environmental sustainability of each configuration using life cycle assessment (LCA). We considered the following design goals for a multistage membrane system: 1) nutrient pre-concentration for down-stream electrochemical struvite recovery, 2) phosphorus removal at early treatment stages, and 3) concentrating nitrogen as liquid organic fertilizer. Synthetic wastewater simulating real wastewater was tested to investigate the nutrient retention performance of the membranes in terms of polymer chemistry and pore size, and to evaluate a range of system designs that would allow the recovery of multiple end-products.

Lastly, electrochemical struvite recovery was performed after the membrane preconcentration of a raw municipal wastewater sample to evaluate the feasibility of electrochemical nutrient recovery from low nutrient raw wastewater sources and highlight the challenges of preconcentration and the downstream struvite production from the concentrated wastewater.

2. Methods and materials

2.1. Preconcentration membrane configurations: design goals for membrane selection

Several membrane configurations were considered for separate or combined nutrient recovery. The selection of membrane type for a specific configuration is based on an anticipated range of performance parameters (i.e., flux, ammonium rejection, phosphate rejection). Fig. 1 shows the potential configuration options for the preconcentration of nutrients in wastewater. Single-stage nanofiltration (Option 1, Fig. 1a) is considered as a concentration step for both ammonium and phosphate nutrients prior to an electrochemical struvite precipitation step, while a two-stage membrane concentration process (Option 2, Fig. 1b) would first concentrate and separate phosphate from the majority of the ammonium, and then the ammonium is concentrated in the second membrane step. Finally, we considered the scenario of a two-stage membrane concentration process before the electrochemical precipitation step, combined with an additional post-electrochemical-reactor ammonium concentration membrane step (Option 3, Fig. 1c), with the goal of producing a highly concentrated aqueous ammonia product stream and a permeate stream with low nutrient content. For the first part of our analysis, we focus on the selection of membranes for Options 1 and 2, while the membrane chosen for ammonia concentration in Option 2 is also utilized in Option 3. The performance efficiency of the membranes was modeled and LCA was used to evaluate the environmental impacts of each configuration.

2.2. Materials

Membrane characteristics of commercially available membranes tested in this study are given in Table 1. Commercial polyamide thin film composite (TFC) membranes (NF90 and BW30LE; DOW FilmTec, Minneapolis, MN), piperazine-amide TFC (TS40; Microdyn-Nadir, Goleta, CA), cellulose acetate (SB90; Microdyn-Nadir), and polyethersulfone (NF030; Microdyn-Nadir) membranes were provided from Sterlitech Inc. (Kent, WA). NFS flat sheet membrane was provided from Synder Filtration (Vacaville, CA). A large pore size polyamide TFC with the commercial name "NF" was obtained from Alfa-Laval (Lund, Sweden). Ammonium chloride (99.99 %, Sigma Aldrich), ammonium dihydrogen phosphate (>98 %, Sigma Aldrich), sodium chloride (>98 %, VWR Chemicals BDH®), sodium hydroxide (ACS grade, VWR Life Science), urea (99.5 %, VWR Life Science), and glucose (99.5 %, VWR Life Science) were used to synthesize membrane system feed solutions. Isopropanol (≥70 %, VWR Chemicals BDH®) was used prior to filtration to wash out impurities from the membranes. Deionized (DI) water was obtained by a Milli-Q ultrapure water system (MA 01730, USA). Raw municipal wastewater was obtained from the Noland Wastewater Treatment Plant (Fayetteville, AR) after the primary grit removal stage. Nessler regent kits and Molybdovanadate reagents were purchased from HACH (Loveland, CO). High purity magnesium (Mg, 99.9 % pure) and stainless-steel (316SS) electrodes were purchased from Goodfellow (Coraopolis, PA).

2.3. Membrane filtration experimental setup

The schematic of the laboratory-scale experimental nanofiltration system used in this study is shown in Fig. 2. The crossflow filtration system is composed of a Delrin membrane cell (CF016, Sterlitech Inc.,

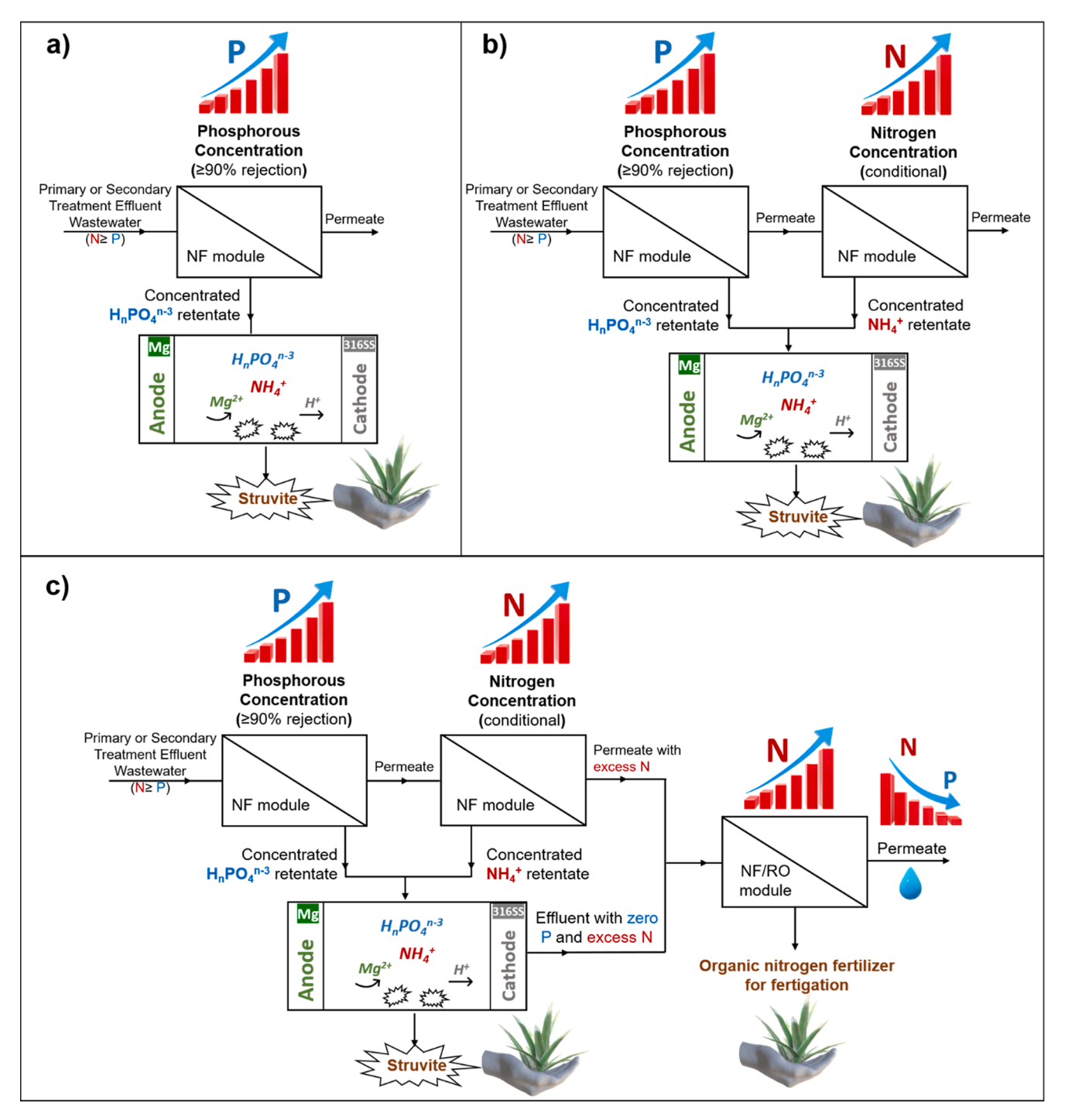


Fig. 1. Three possible system configurations for nutrient recovery depending on the relative levels of N and P in source wastewater are presented: a) a single-stage nanofiltration, b) a two-stage nanofiltration, and c) a multi-stage membrane concentration process with a post-electrochemical concentration for excess N recovery.

Kent, WA) connected to a conical stainless-steel feed tank with cooling coils inside connected to a heat exchanger (Pharmacia Biotech, Uppsala, Sweden) to maintain a constant temperature during the pressure-driven filtration. A high-pressure pump (Wanner Engineering, Inc., Minneapolis, MN) with a brass head and Teflon tubing were used to pump the feed water. The retentate was recycled back to the feed tank, and the permeate was collected in a tank on balance (Mettler Toledo, Columbus, OH). The cell membrane area was 20.6 cm². Before the experiment, the fresh commercial membrane was immersed in DI water for about 24 hr., followed by washing for 1 min with 30 % isopropyl alcohol to remove impurities on the membrane surface. Before installing the membrane, the system was washed with a NaOH solution (pH 10.30), followed by

rinsing with DI water. The feed flow rate was monitored by a flowmeter applied to the recycle line. Prior to each test, membranes were pressurized with DI water for one hour, under the same conditions as the subsequent test, to reach a stable flux. The water flux of the membranes was measured by recording the rate of weight change on the permeate side with a digital scale. Flux decline index was calculated for each membrane by the following formula:

$$Flux DeclineIndex = \frac{J_w - J_P}{J_w} \tag{1}$$

where $J_w(LMH)$ is pure water flux and $J_P(LMH)$ is effluent permeate flux

Table 1
Membrane characteristics of the commercial membranes used in this study.

Provider	DOW Filmtec	Sydner Filtration	TriSep	DOW Filmtec	TriSep	Alfa Laval	Microdyn-Nadir
Name	BW30LE	NFS	SB90	NF90	TS40	NF	NF030
Name in this	BW30LE	Synder	SB90	NF90	TS40	Alfa	NF030
study							
Type/	Thin film	Thin film	Nano-filtration/	Thin film	Thin film	Thin film	Nano-filtration/
active layer	composite/	composite	Cellulose	composite/	composite/	composite	Polyethersulfone
	Polyamide		acetate	Polyamide	Piperazine-amide		
MWCO (Da)	100	100-250	150	200-400	200-300	300	500
Contact angle (°)	$\textbf{42} \pm \textbf{4} \; \textbf{[17]}$	25-30*	59 ± 2.75 [18]	52 [19]	22 [19]	49 [19]	55.17 ± 2.71 [18]
Rejection	99 % NaCl	50 % NaCl	85 % NaCl	99 % MgSO ₄	$\geq\!98.5~\%~MgSO_4$	$\geq\!98~\%~MgSO_4$	80-95 % Na ₂ SO ₄

^{*}Synder Filtration.

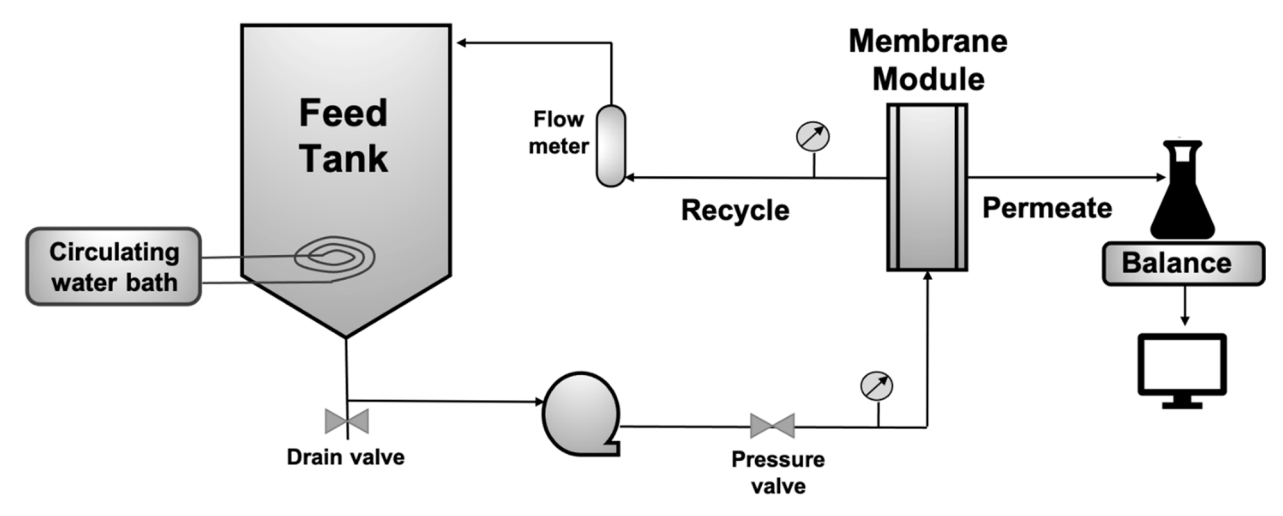


Fig. 2. Cross-flow membrane filtration system.

after 10 h filtration.

Two batches of experiments, short-term and long-term, were designed to analyze the performance of the commercial membranes. In short-term studies, all commercial membranes were tested by filtering synthetic wastewater with three different concentrations of ammonia and phosphate to down select the membranes based on the retention efficiencies. The filtration duration was 2 h in the short-term studies and 10 h in long-term studies. For all membranes, a constant transmembrane pressure (TMP) of 5 bar and a flow rate of 1 L min⁻¹ was maintained. In long-term studies, the BW30LE membrane was tested at both 5 and 20 bar TMP to compare BW30LE membrane performance to NF membranes as well as to include a condition closer to the conditions of RO mode operation in a full-scale system. Two liters of feed solution were used in all experiments except for the test 'BW30LE- 20 bar' due to the high water permeation flux and to avoid evacuation of the feed tank during the long-term test.

2.4. Electrochemical reactor setup and electrolysis experiments

The electrochemical experiments were carried out at room temperature (rt) in a single-compartment reactor, as described in our previous studies [6]. The batch reactor was filled with $\sim450~\text{mL}$ of membrane pre-concentrated real wastewater and continuously stirred at $\sim200~\text{rpm}$, where a magnesium plate (Mg, 99.9 % pure) served as the anode and a stainless-steel plate (316SS) as the cathode, while an output precision variable digital power supply from Yescom provided a constant potential ($\sim31~\text{V}$) for the reaction. The 25 cm² size plates with an active surface area of $\sim40~\text{cm}^2$ (both sides of the electrodes were used) were separated by 5 cm. The precipitates formed on the anode and cathode were collected by scraping the electrode carefully with a razor and were dried at room temperature. The plates were cleaned with different grain

size abrasive paper (Norton Abrasives), purchased at a local hardware store.

2.5. Synthetic wastewater composition

The average nitrogen to phosphorus mole ratio (N/P) for most real wastewater sources is reported in the range of about 10–20 in the literature [20–22]. Here, the N/P mole ratio was set near to 10 for all the synthetic water compositions. In short-term studies, membranes were tested with three different water compositions. The pH of the solution was adjusted to 7, using a 0.5 M sodium hydroxide solution. Total dissolved solids (TDS) of the synthetic water were held constant for all the experiments using sodium chloride to avoid the effect of variable TDS on the membrane performance. In long-term studies, synthetic wastewater was prepared in a more complex matrix compared to the short-term studies to simulate the characteristics of real wastewater sources. The composition of the synthetic solution is given in Table 2. N/P ratio was 10 in the long-term studies. Glucose and urea were added to include chemical oxygen demand (COD) and organic nitrogen as total Kjeldahl nitrogen (TKN) concentrations in the wastewater matrix. Table 2 shows

Table 2 Synthetic wastewater composition.

Wastewater Parameters	Short-te	rm Studie	Long-term Studies	
	Test 1	Test 2	Test 3	Synthetic wastewater
NH ₄ -N (ppm)	10	200	1000	48
PO ₄ -P (ppm)	2.5	50	252	10.6
Conductivity (µs/Cm)	4950			1320
pН	7			7.4
COD (ppm)	-			314
TKN (ppm)	-			53

the composition of the synthetic wastewater for the two batches of experiments.

2.6. Water chemistry analysis

Ammonium and phosphate ion concentrations of wastewater samples were characterized by colorimetric methods using HACH Nessler and Molybdovanadate reagents, respectively. Three measurements were conducted per sample, and results are reported as the average of the measured values and the error bars represent the standard deviation. COD was measured by a DR900 multiparameter portable colorimeter obtained from HACH Company (Loveland, CO) after preparing the samples with a COD measurement kit from CHEMetrics Inc. (Midland, VA). Rejection efficiencies were calculated from Equation (2):

$$Rejection(\%) = (\frac{C_f - C_p}{C_f}) \times 100$$
 (2)

where C_p and C_f are the concentrations in the permeate and feed streams, respectively. TKN measurement was performed by Arkansas Water Research Center (Fayetteville, Arkansas) using the catalytic combustion method [23].

The concentration factor for all measured water parameters was calculated by the following equation:

$$Concentration factor = \frac{C_{initial}}{C_{final}}$$
 (3)

where $C_{initial}$ (mg/L) and C_{Final} (mg/L) are concentration of parameters before and after concentration, respectively.

2.7. Membrane characterization

Membrane surfaces before and after filtration were analyzed using a Nova Nanolab 200 Duo-Beam SEM instrument (FEI, Hillsboro, OR). Membrane samples were prepared prior to imaging by drying in a vacuum oven at 40 $^{\circ}\text{C}$ for 2 hr and coating a gold layer to provide an electrically conductive surface. A PerkinElmer Frontier Fourier-transform infrared spectrometer (FTIR) was used to analyze the membrane fouling on the surface. FTIR analysis was conducted using infrared light with an average of twenty scans from 4000 cm $^{-1}$ to 650 cm $^{-1}$. The surface morphology of membranes was measured using a 3D Laser Scanning Confocal Microscope (KEYENCE Corporation, Tokyo, Japan). Surface roughness values are reported as an average of three measurements from different areas of the samples. The crystal structure of the solids formed on the anode and cathode were carefully collected and analyzed via X-ray diffraction (XRD) on a Philips PW1830 double system diffractometer equipped with a Cu cathode.

2.8. Life cycle assessment

A life cycle assessment for five scenarios was conducted based on the three preconcentration membrane configurations shown in Fig. 1. The first two scenarios were chosen based on the configuration of Option 1—one scenario utilized the membrane that showed the highest phosphate-concentrating potential from the long-term studies and a second scenario that utilized the membrane with the highest ammonium-concentrating potential. A third scenario was based on the configuration of Option 2, with the previously chosen membranes providing two-stage filtration (phosphate concentration followed by ammonium concentration). A fourth scenario followed the configuration of Option 2 with the exception that the retentate from the second filtration step, a concentrated NH3 stream, was utilized directly as a fertilizer substitute instead of being directed towards electrochemical struvite precipitation. In this fourth scenario, the permeate from the second filtration step was directed towards struvite recovery. A fifth scenario followed the configuration of Option 3, again with the chosen

membranes providing three-stage filtration (one phosphate-concentrating membrane followed by two ammonium-concentrating membranes). Process flow diagrams are available for each scenario in the Supplementary Material (Fig. S.1, Electronic Supplementary Information (ESI)). These configurations were built and simulated in Super-Pro Designer®. The lifecycle inventory (LCI) produced from the simulations was transferred to SimaPro® for full lifecycle impact assessment using the Ecoinvent V3.7 consequential system model for upstream production processes and avoided fertilizer production impact [24].

2.8.1. LCA goal and scope

The goal of this analysis was to provide a comparison of the environmental impacts of each preconcentration configuration and provide insight into the potential environmental benefits of membrane and struvite recovery technology in wastewater treatment. The system boundary used for this analysis included all materials and energy needed for membrane manufacturing, membrane filtration operation, electrode processing, electrochemical cell operation, drying of wet struvite, disposal of used materials, and environmental benefits resulting from the production of struvite and substituting commercial fertilizers. This system boundary did not include any pre- or post-treatment steps present in a typical wastewater treatment plant; only preconcentration and struvite recovery steps were included in this analysis. The functional unit for this study was chosen to be treatment of 1 m³ of synthetic wastewater.

2.8.2. Life cycle inventory

Process simulations for all treatment options shown in Fig. 1 were built in SuperPro Designer. Membrane filtration steps were added in the simulation with influent composition reflecting that of the experimental synthetic wastewater used in the long-term studies (Table 2). All simulations were built assuming steady-state operation. The reference flow rate for each option modeled was the treatment of 1 million gallons per day (MGD). Inputs for each filtration step, including the concentration factor, volume reduction factor (VRF), rejection coefficients, and average flux achieved, were based on experimental data gathered from the long-term studies. Pumping energy was calculated based on the volumetric flow rate going into each membrane and an assumed pressure drop of 5 bar. A membrane lifespan of five years was assumed for all membranes. End-of-life (EoL) modeling for each membrane and the stainless-steel electrode was included in our LCI using existing Ecoinvent disposal processes. Membrane disposal was modeled as mixed plastic waste disposed in a sanitary landfill. Disposal of the stainless-steel electrode was modeled as scrap steel disposed in a sanitary landfill. EoL modeling for the magnesium was not included in our LCI. Our decision to exclude EoL modeling of magnesium from our LCI is intended to provide conservative estimates for environmental burdens of the magnesium anode as described below. The production of primary magnesium is an energy intensive process, and efforts exist to create cost-effective processes to recycle magnesium for reuse (i.e., its reutilization in producing aluminum alloys for vehicles, etc.) [25-26]. The inclusion of magnesium recycling in our process would provide environmental credits from offsets in primary magnesium production. Thus, exclusion of EoL modeling for magnesium provides life cycle impact assessment (LCIA) results that are more conservative compared to a scenario with Mg recycling. Struvite recovery was based on the stoichiometry of the struvite precipitation reaction and a 90 % extent of reaction was assumed. Materials and energy required for electrochemical precipitation were modeled based on experimental results reported in Kekedy-Nagy et al. [27] and scaled up for the SuperPro simulations. Material and energy requirements estimated from experimental and modeling results for all processes included in the system boundary comprised our life cycle inventory. This data is provided for each scenario in the Supplementary Material (Table S.1, ESI). As struvite and/or a concentrated NH3 stream was produced in each scenario, an

avoided burden (i.e., environmental credit) was given for these fertilizer substitutes produced in each of the options modeled. Avoided burdens from fertilizer substitutes were accounted in the LCI model in the SimaPro platform as kg of phosphate fertilizer, as P_2O_5 , and kg of ammonium nitrate, as N, equivalent to the P and N provided by struvite and the concentrated NH $_3$ stream.

2.8.3. Life cycle impact assessment

An LCIA in SimaPro 9.0 was generated based on the life cycle inventory model described above for the functional unit of the treatment of 1 $\rm m^3$ of wastewater. TRACI v.2.2 was used as the impact methodology to generate a comparative life cycle impact assessment for each of the preconcentration options. These results were normalized based on the highest impact for each category and are shown in Section 3.5.

3. Results and discussion

3.1. Commercial membranes performance analysis for nutrient preconcentration

Membranes were tested with different compositions of synthetic water to investigate the ammonia and phosphate rejection efficiencies and the effect of nutrient concentration on membrane performance. The most promising membranes were then selected for further investigation in long-term studies. The permeance flux of membranes is shown in Fig. 3 and Fig. S.2. Results indicate that, in general, polyamide thin film composite nanofiltration membranes have higher fluxes than the other membranes. The ultrathin selective layer on the top of the polyamide thin film composite facilitates high permeate flow at low pressures. The BW30LE reverse osmosis membrane had a lower flux compared to nanofiltration polyamide TFC membranes due to the dense active layer on top [28]. The lower flux of SB90 and NF030 membranes can be attributed to the lower hydrophilicity characteristic of cellulose acetate and PES surfaces, with thus less interaction of water molecules with the membrane active layer [18]. Cellulose acetate membranes with a thick active skin layer (e.g., 100-1000 nm) have a lower wastewater flux than polyamide TFC membranes, which have an ultra-thin active layer (e.g., 20-200 nm) [29].

Filtration samples were collected from the feed and permeate side every half an hour for each experiment. Ammonium and phosphate rejection efficiencies were measured for membranes after each test, and the average and standard deviation of rejection efficiency is given for each condition in Fig. 4. As expected, the BW30LE membrane with a denser active layer had the highest solute selectivity for all three conditions. Synder, NF90, and Alfa are nanofiltration polyamide-TFC membranes with high divalent ion rejections. Therefore, phosphate

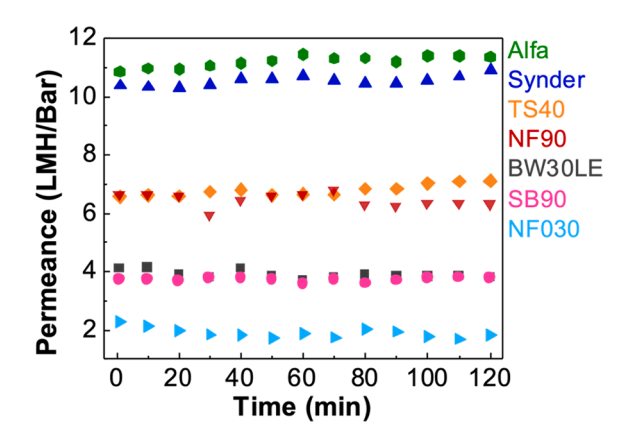


Fig. 3. Measured membrane permeance flux during filtration of a synthetic solution with NH_4^+ and PO_4^{3-} concentrations of 1000 ppm and 252 ppm, respectively.

ion is rejected efficiently by these membranes through the size exclusion mechanism. Synder and NF90 had similar (slightly higher for NF90) ammonium rejection efficiency. The rejection mechanism can be considered as both size exclusion and Donnan exclusion as these membranes have functional groups on the surface that, in addition to their tight active layer, may cause the repulsion of ammonium ions [30-31]. SB90 and TS40 membranes showed a high phosphate rejection but lower ammonium rejection. The cellulose acetate membrane has a less negatively charged surface than polyamide TFC membranes which causes this membrane to have less solute rejection and selectivity [32-33]. It can also be seen in Fig. 4 that despite the higher MWCO of TS40 compared to SB90, ammonium rejection efficiency is higher for the TS40 membrane, which has a polyamide surface. Among polyamide membranes, NF90 and BW30LE were more stable in ammonium rejection rates across the tested concentrations. These membranes contain a fully aromatic polyamide top layer with a high surface roughness due to a "peak and valley" structure (see Fig. 5 and Table S.2) that can provide a very high rejection rate through size and Donnan exclusion. At higher concentrations, the ammonium rejection was decreased for Synder and TS40 (Fig. 4a), while phosphate rejection remained efficient (Fig. 4b). The decrease in ammonium rejection can be due to a decrease in the Donnan effect as the smaller ions are mainly rejected by the Donnan exclusion mechanism. The surface of Synder and TS40 membranes are composed of a semi-aromatic polyamide active layer (see Fig. 5), and accumulation of ions at the surface can induce a charge screening effect of the counter-ions leading to a decrease in repulsive forces and the Donnan effect [34]. However, the active layer of the membrane surface has effectively rejected phosphate ions with a larger hydrated ionic radius through a size exclusion mechanism.

3.2. Membrane down-selection and characterization

The best-performing membranes were chosen based on the rejection efficiency of the two nutrient species and the permeate flux. BW30LE, Synder, and NF90 membranes were selected for testing in long-term studies due to higher ammonium rejections. The long-term operation of the Alfa membrane was also considered since it showed high water permeate flux and a high phosphate selectivity, indicating that this membrane has suitable characteristics for a single-step phosphorus preconcentration. Considering that N/P ratios are often higher than 10 in real wastewater sources [20–22], concentrating phosphorus as the limiting element can help enhance recovery at down-stream operations.

FTIR spectra of pristine membranes are shown in Fig. 5. The FTIR of fully aromatic and semi-aromatic polyamide membranes is fully discussed by Tang et al., [35] where the authors demonstrated that semiaromatic polyamide membranes have a slightly different FTIR spectrum compared to fully aromatic polyamide membranes. The absence of an aromatic amide band (N-H deformation vibration or C=C ring stretching vibration) at 1609 cm⁻¹ and an amide II band (N—H in-plane bending and N—C stretching vibration of a —CO—NH— group) at 1541 cm⁻¹, and the presence of an amide I band for poly(piperazinamide) at 1630 cm⁻¹, show the semi-aromatic nature of Alfa and Synder membrane surfaces. Fig. 3 shows that the Alfa membrane had the highest wastewater flux among the membranes, which is due to the loose active layer and the nature of the polyamide chemistry on the surface. NF90 and BW30LE are composed of a dense fully aromatic polyamide layer on the top, which causes a lower wastewater flux but higher rejection. The reduced aromaticity of Alfa and Synder membranes results in a more hydrophilic and less selective surface compared to NF90 and BW30LE membranes.

3.3. Long-term flux and rejection analysis for selected membranes

The four down-selected polyamide TFC membranes were tested with synthetic wastewater to evaluate the rejection efficiency and flux stability in a longer-term filtration study. Membrane permeance fluxes in

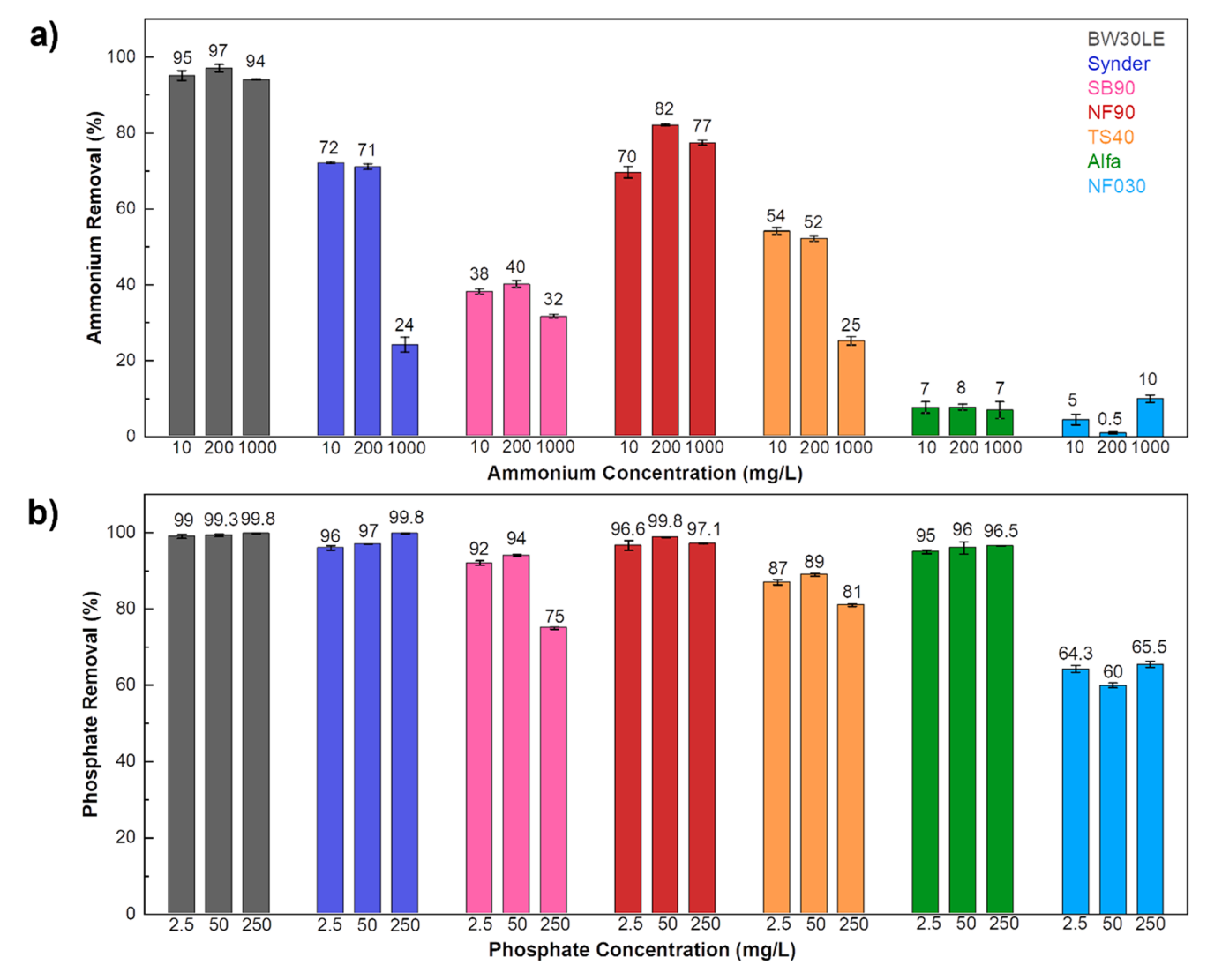


Fig. 4. Membrane rejection efficiency at three different concentrations of a) ammonium and b) phosphate as a function of membrane type.

long-term filtration studies are shown in Fig. 6a. Fig. 6b shows the flux decline index for the down-selected membranes after 10 hr. All the membranes became fouled and exhibited flux decline to some extent. FTIR spectra of tested membranes (Fig. S.3, ESI) showed peaks related to urea and glucose, indicating the organic fouling on all the membrane surfaces. However, Alfa and Synder membrane fluxes were more stable than NF90 and BW30LE membranes.

Fig. 7 (a) shows ammonium, phosphate, COD, and TKN rejection for all four of the tested membranes. Ion rejection efficiencies were similar to the short-term results for all the membranes. COD and TKN of the synthetic water were rejected better by BW30LE and NF90 membranes, and the rejection mechanism is likely through size exclusion based on the comparative hydrated molecular sizes of the wastewater matrix components and the reported MWCOs of the two membranes. Fully aromatic membranes have higher rejection due to the denser and thicker active layer compared to semi-aromatic membranes [36]. However, as mentioned above, the dense and rough surface of fully aromatic membranes causes a higher extent of organic foulant absorption [35]. Therefore, BW30LE or NF90 are more functional for treating a wastewater source with low organic compound composition, such as municipal wastewater or sea water, where there is less organic fouling potential. Conversely, semi-aromatic membranes with a smoother and more hydrophilic surface can effectively concentrate animal or industrial wastewater with a high organic compound composition (refer to Table S.2. for surface roughness values).

The concentration factor for all water parameters is shown in Fig. 7 (b). COD and TKN concentration factors were investigated to evaluate the feasibility of recovering ammonium as an organic nitrogen fertilizer and ammonium concentration in the presence of organic carbon in down-stream operations. BW30LE membrane rejection efficiency was not affected by the increase in pressure; however, the lower pressure resulted in a low water permeation flux (LMH) and VRF (42 % at 20 bar and 24 % at 5 bar), resulting in a lower concentration of wastewater. Synder and NF90 showed similar concentration factors for ammonium and phosphorus. Although NF90 had a slightly higher ammonium rejection, the flux decline throughout the filtration study caused the final concentration factor to be similar to that of the Synder membrane. The Alfa membrane provided low ammonium and organic nitrogen concentration factors. The high MWCO for this membrane can allow the passage of small species through the membrane. However, Alfa membrane yielded the highest phosphate concentration in the final feed stream due to the high phosphorus rejection rate and volume reduction factor (60 %) resulting from the high wastewater flux. COD and TKN concentration factors are higher for BW30LE at 20 bar and NF90 membranes due to the higher rejection rates and potentially due to higher organic foulant adsorption of these membranes. The SEM imaging results of the membranes after filtration (Fig. S.4, ESI) also confirms a higher extent of fouling on the surface of BW30LE and NF90 compared $\,$

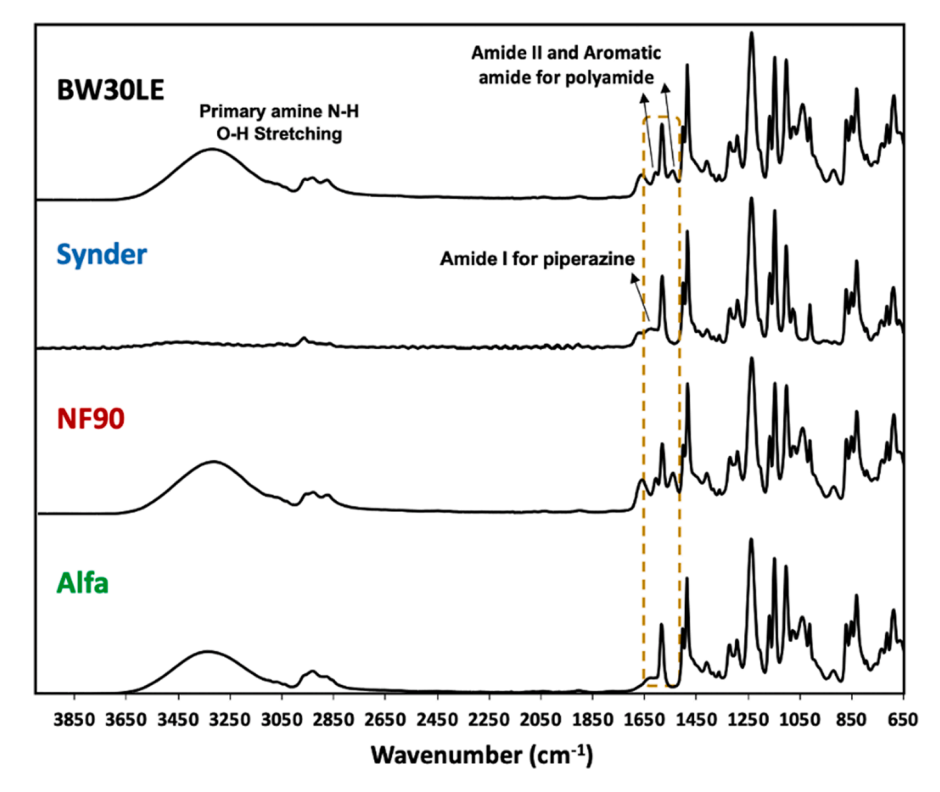


Fig. 5. FTIR spectra of down-selected membranes.

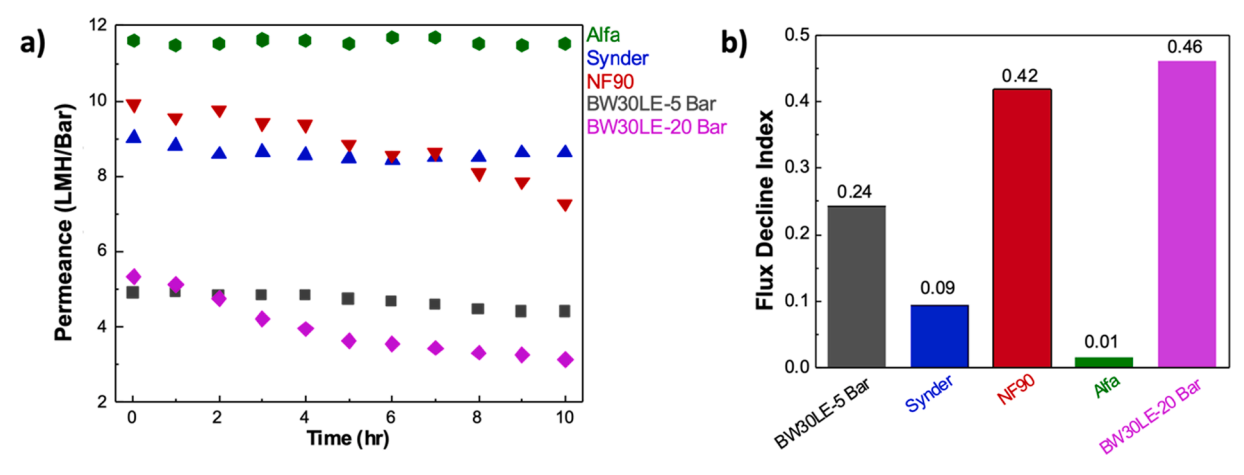


Fig. 6. A) Synthetic wastewater permeance flux and b) flux decline index after 10 hr. filtration for the selected membranes.

to Alfa and Synder membranes, which agrees with flux decline results in Fig. 6b. The surface roughness results (Table S.2, ESI) indicate that fully aromatic pristine membranes have higher surface roughness with a "peak and valley" structure compared to the smooth surface of semi-aromatic pristine membranes. A higher density of peaks and valleys can be seen on BW30LW and NF90 in Fig. S.5, ESI. The 3D laser images after filtration shows that the valleys are mostly clogged after filtration due to surface fouling.

These results give more insight into selecting an appropriate membrane for the different process options presented in Fig. 1. The Alfa membrane, with the highest concentration factor, can be highly efficient in P recovery from wastewater in a single stage or as the first stage in a two-stage nanofiltration system, where in the second stage, NF90 or Synder membranes can be used to concentrate N in the wastewater. In the third membrane filtration stage, where the excess of nitrogen left in the previous streams is concentrated, NF90 or BW30LE with a high N

rejection % would be efficient in the recovery of nitrogen. These two membranes possess a low MWCO and a highly selective top layer that helps the retention of ammonium ions.

3.4. Life cycle impact assessment of multi-stage membrane design using the selected membranes

Based on membrane performance in the long-term studies, the phosphate-concentrating membrane, Alfa, and ammonium-concentrating membrane, NF90, were chosen as the preconcentration membranes that would be modeled for each scenario based on the configurations in Fig. 1. Fig. 8 shows the life cycle impact assessment results for each scenario using these membranes grouped by impact categories. Process contribution results are presented for each scenario with groups of unit processes that contributed to each impact category (i.e., electricity, electrode manufacturing, etc.). These process

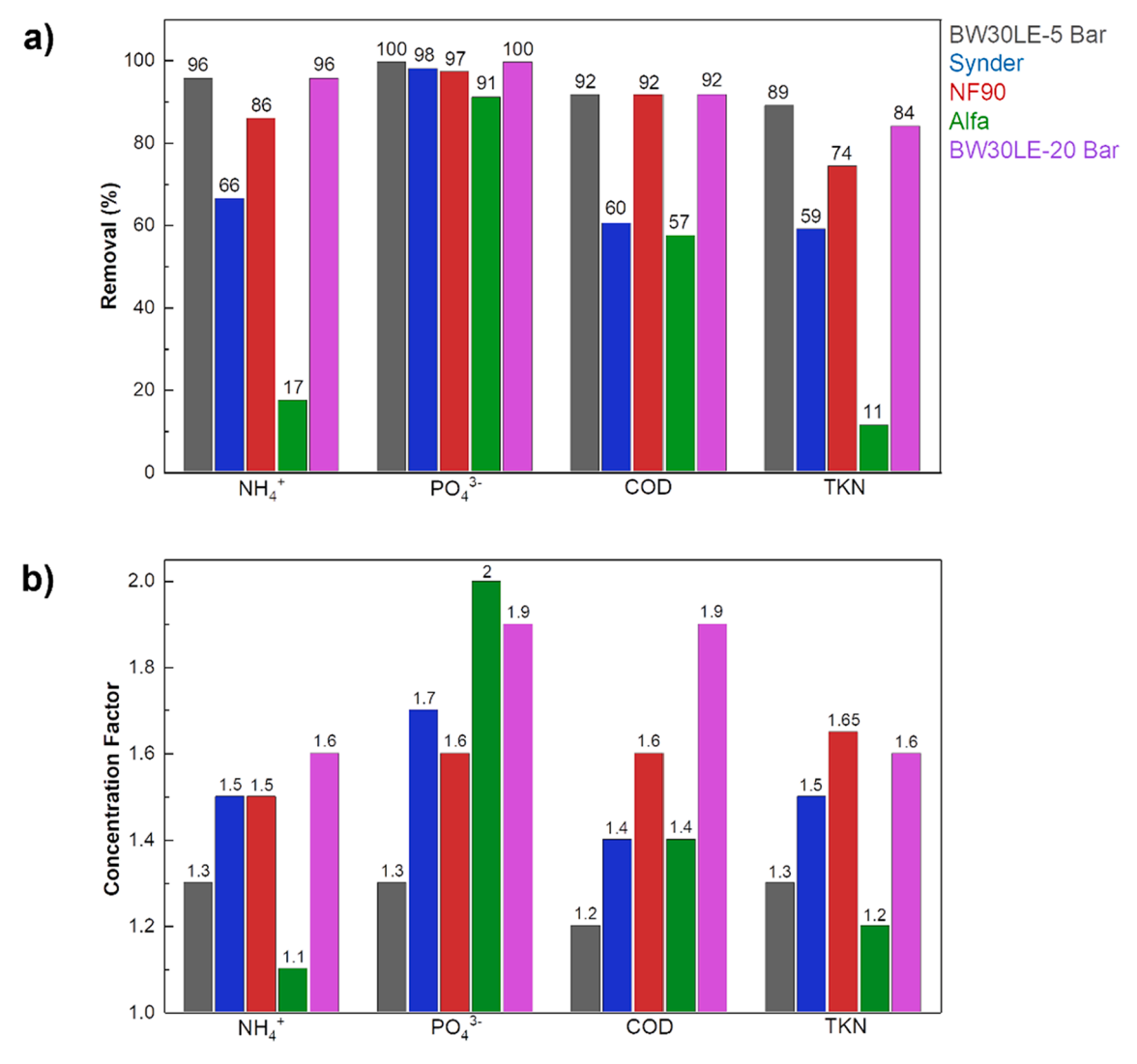


Fig. 7. A) Long-term filtration membranes rejection efficiencies, and b) final feed concentration factors for the measured parameters after 10 h filtration. An initial feed volume of 2L was used for all membranes at 5 bar. An initial feed volume of 4L was used for BW30LE at 20 bar.

contributions are shown as different colored bars within each bar for each scenario. Total midpoint environmental impacts for each scenario are also presented (as red dots) the left and right axes with corresponding units (e.g., kg CO₂-equivalent for global warming potential) labeled on the horizontal axis.

Fig. 8 shows that electricity, which included pumping, electrochemical precipitation, and struvite drying energy, was the largest contributor for every scenario in all impact categories, accounting for approximately 38-96 % of the overall impact. Electrode manufacturing, including materials and energy needed for both Mg and stainless-steel electrodes, accounted for 4-43 % of the overall impact for all scenarios. Struvite and the concentrated ammonia stream recovery provided environmental credits ranging from 3 to 57 %, with higher credits achieved from Option 2-Modified and Option 3 across all categories except for acidification and respiratory effects. In the eutrophication potential category, Option 1-Alfa and Option 1-NF90 had 47 % and 10 %of impacts, respectively, stemming from residual nutrients in the effluent that were released to water ('Other' category). While membrane manufacturing was included in our life cycle inventory, the relative impact of this step was negligible compared to electricity used and electrode production for each scenario. In overall total impacts, Option 1-Alfa, followed closely by Option 1-NF90, had the lowest total midpoint impacts in the categories of ozone depletion (40 % relative impact to the scenario with the highest ozone depletion), global warming potential

(46 %), smog (46 %), acidification (30 %), carcinogenics (39 %), respiratory effects (46 %) and fossil fuel depletion (43 %). Option 1-NF90 had the lowest total impact in eutrophication (57 %). Option 2-Modified had the lowest total impact in non-carcinogenics (23 %) and ecotoxicity (-29 %).

SuperPro simulations showed the amount of struvite produced from each scenario did not vary significantly between the different configurations; the amount of struvite produced, assuming a treatment of 1 MGD of wastewater, varied between approximately 103-113 kg struvite per day. The small range of struvite produced across the different configurations resulted from a limited amount of initial phosphate ions compared to ammonium ions in the influent synthetic wastewater, making phosphate the limiting factor in the electrochemical reactor for all scenarios. However, an additional fertilizer substitute, the concentrated ammonia stream, was produced in Option 2-Modified and Option 3. The production of the additional fertilizer substitute in Option 2-Modified and Option 3 correlated with the higher environmental benefits observed from fertilizer across all impact categories except acidification. Unlike the results for all other scenarios, struvite recovery for Option 2-Modified and Option 3 incurred environmental burdens as opposed to environmental credits. An increase in acidification impacts was found to originate from a market mediated effect in the metals production sector related to fertilizer production. Specifically, production of ammonium nitrate consumes nitric acid. Nitric acid production

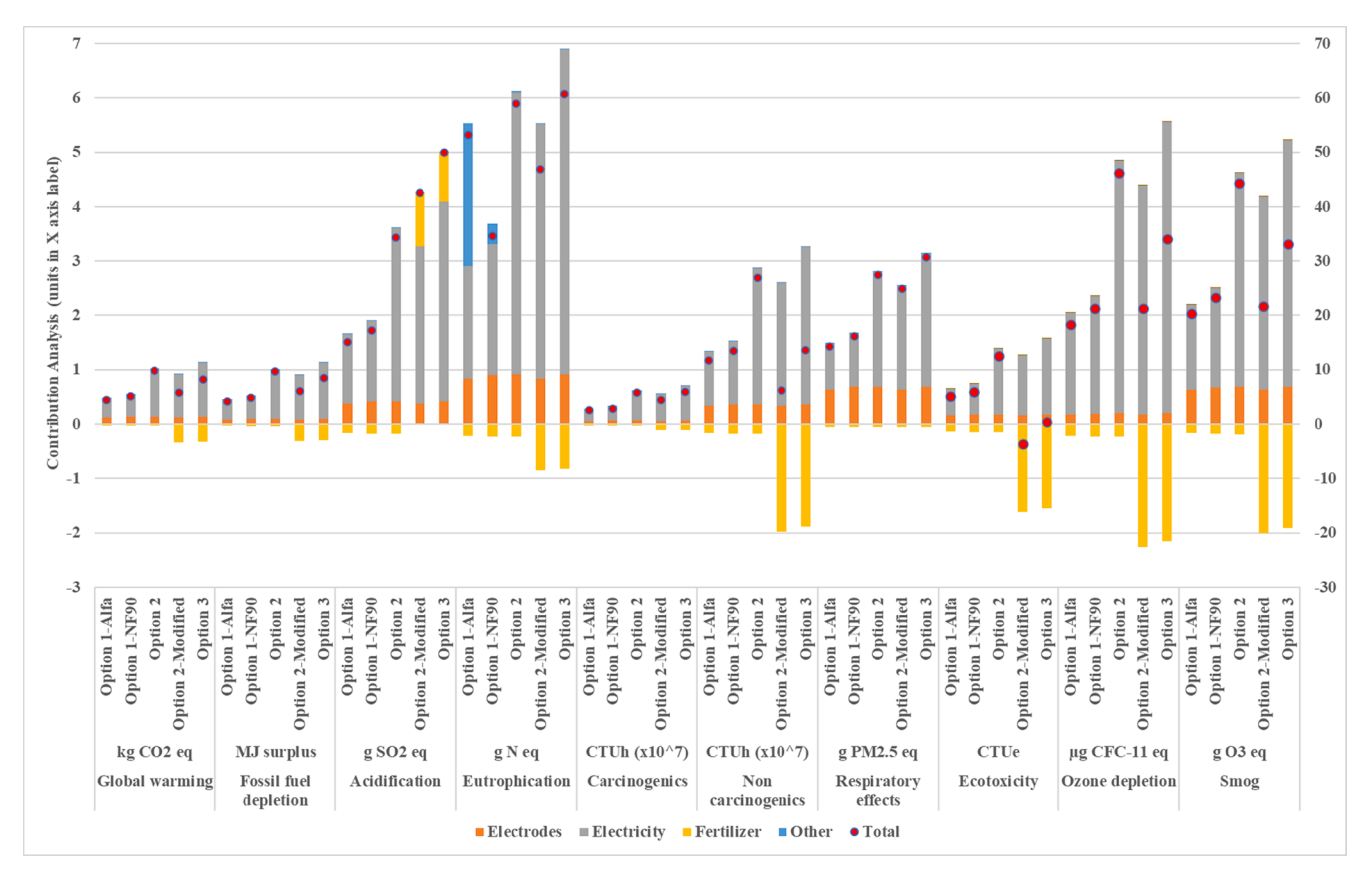


Fig. 8. LCIA results and process contribution for the five scenarios: Option 1-Alfa, Option 1-NF90, Option 2, Option 2-Modified, and Option 3.

consumes platinum. Copper, gold and nickel are co-produced with platinum, and the reduction in platinum demand from substituting ammonium nitrate lowers the amount of these co-produced metals, which are then supplied from more impactful processes; thus, reduced production of ammonium nitrate leads to larger impacts in nonplatinum metal extraction industries. Across all but two categories, Options 2 and 3 had the largest burdens compared to all other scenarios, demonstrating that total environmental impact tended to increase as the number of membranes used in the process increased. These results are consistent with the observation that pumping energy, the largest contributor to the 'Electricity' group for all scenarios, increased as the number of membranes added to each configuration increased. Option 2-Modified, while it also utilized multiple membranes, had lower impacts than Options 2 and 3 in all categories except acidification due to the environmental credit received from offsetting synthetic fertilizer production.

Between the two scenarios that only utilized one membrane in the process, Option 1-Alfa had lower impacts than Option 1-NF90 in all categories except eutrophication. Life cycle inventory values show that more energy was used for pumping wastewater through the NF90 membrane than that of the Alfa—higher VRFs (retentate to feed) for the NF90 membrane compared to the Alfa membrane resulted in a larger volume of wastewater being recycled throughout the system. Thus, a higher volume of wastewater was pumped through the NF90 membrane compared to that of the Alfa. While Option 1-Alfa is the scenario with the lowest impact for almost all impact categories, Option 1-NF90 and Option 2-Modified have lower total impacts than Option 1-Alfa for the categories of eutrophication, and non-carcinogenics and ecotoxicity, respectively. In eutrophication potential, Option 1-NF90 released 3.5 g N-equivalent, while all other scenarios released between 4.7 and 6.1 g Nequivalent for the same functional unit. For all other scenarios except Option 1-Alfa, these results are consistent with the observation that added membranes increased the total impact of the system. Process

contribution results show nutrients released to water from effluent, as phosphate and ammonia, contributed 2.6 g N-equivalent (49 %) to overall eutrophication impacts for Option 1-Alfa. The NF90 membrane had a higher phosphate rejection rate (97 %) compared to the Alfa membrane (91 %), therefore Option 1-NF90 filtered out more phosphate that was then available for struvite precipitation. Lastly, Option 2-Modified showed the lowest total impacts for non-carcinogenics and ecotoxicity. Process contributions showed that the environmental benefit of producing struvite and the concentrated NH₃ stream in Option 2-Modified reconciled the increased impacts from electricity of utilizing two membranes as opposed to one. Overall, while impacts from membrane fabrication were found to be negligible, membrane operation contributed significantly to the environmental performance of each scenario studied. In this case where struvite production is limited by influent concentration of phosphate, the addition of membranes does not result in increased struvite production. As a result, the environmental impacts for scenarios in Options 2 and 3 were mostly higher than those for singlestage filtration. Some exceptions to this trend indicate how increased impacts from the addition of membranes could be partially offset by reducing nutrient content in the effluent and increasing fertilizer production at the wastewater facility. Thus, in situations where the phosphate and ammonia influent concentrations are more closely balanced for the production of struvite, it is possible that the substitution of more synthetic fertilizer would improve the performance of multi-membrane options. It is also reasonable to anticipate that adoption of renewable electricity for the operation of pumps would lead to better results for systems with more membranes.

3.5. Challenges and opportunities of nutrient recovery from real wastewater

A single step membrane preconcentration step followed by an electrochemical reactor as the struvite production step, was carried out to

investigate the nutrient recovery from real wastewater including the challenges and opportunities for further investigation (Fig. S.6, ESI). A raw municipal wastewater stream was selected with no pretreatment. The wastewater composition is shown in Table 3. The NF90 membrane was selected for the preconcentration of nutrients in municipal wastewater due to the high ammonium and phosphorus retention efficiencies. NF90 was chosen due to the high rejection efficiency and the more stable flux compared to BW30LE. This membrane might also enable lower cost operation than the BW30LE membrane (due to lower operating pressures) with a lower flux decline and higher ammonium concentration efficiency than Synder and Alfa membranes.

The NF90 membrane was tested for 10 h under 5 bar TMP and 1 L. $\rm min^{-1}$ flowrate to concentrate nutrients in wastewater. Then, the membrane was cleaned by cycling DI water through the system under the same pressure and flow rate for one hour. The cleaned-membrane pure water flux was measured by running DI water through the membrane for 10 min. The DI water was drained, and concentrated wastewater was again placed into the feed tank for the second preconcentration run.

Since raw municipal wastewater including suspended solids was used as the influent for the preconcentration step, suspended solid particles deposited within the nanofiltration system during operation, fouling the membrane and the filtration system. Although the membrane rejected nutrients with high rejection efficiencies, the wastewater nutrient concentration of the concentrate was lower than the influent. This result can be attributed to the retention of nutrients in the suspended solid particles deposited in the system or the precipitation of nutrients in the system [37]. This result suggests the need for an ultrafiltration system as the pretreatment system to remove total suspended solids from the municipal wastewater prior to the nanofiltration system, as well as a pH control strategy or the use of antiscalants to avoid the precipitation of nutrients in the preconcentration step [38].

A decrease in the initial flux and a large flux decline were observed compared to the synthetic wastewater flux (Fig. 6), which is likely due to the presence of suspended solid particles in municipal wastewater (Fig. S.7, ESI). The membrane cleaning was not efficient, and more frequent cleaning is likely required to recover the water flux of the membrane. The membrane flux was more stable in the second membrane filtration period. Flux decline was mainly due to the organic fouling resulting from the presence of suspended solids in the wastewater. An early chemical cleaning might help to avoid irreversible organic fouling on the membrane surface.

The concentrate stream after the second preconcentration step was collected from the membrane system and placed in a single-cell electrochemical batch reactor (Fig. S.8, ESI), where a sacrificial magnesium electrode was used as the only source for Mg, with no pH adjustment, to investigate the potential recovery of nutrients as struvite. The pH of the bulk wastewater solution increased from an initial pH of 8.1 ± 0.2 to 11.2 ± 0.2 during the 7 h testing period, while the measured current increased from 0.1 ± 0.0 to 0.2 ± 0.01 A, respectively, and the energy consumption was ~0.1 kWh. The current increase over time suggests an increase in Mg corrosion, which may have been driven by precipitation reactions and changes in passivation and fouling at the electrode

Table 3The major ionic composition is determined in raw wastewater, preconcentrated wastewater, and electrochemical reactor effluent, respectively, and the ion removal efficiency (%).

Parameters (ppm)	Raw wastewater	Preconcentration effluent	Electrochemical reactor effluent	Removal (%)
PO ₄ ³⁻	1.5	1.2	0	100
NH_4^+	27.7	15	10.4	30
Cl-	40	48	7.2	85
NO_3^-	2.4	2.1	n.d. ^a	100
NO ₃ SO ₄ ²⁻	50	50	20	59

^a Not detected.

surface. It should be noted that the temperature of the test solution increased from room temperature to \sim 37 $^{\circ}C$ as a result of electrochemical Mg corrosion.

The pure-Mg anode (see Fig. S.8, ESI) sustained significant morphological changes during electrochemical operation in the form of corrosion and fouling, which is the result of the harsh environment delivered by the composition of the real wastewater. The concentration changes of the major anions and cations present in the raw wastewater, as determined by spectrophotometric analysis and ion chromatography, after the preconcentration step and after the 7-hour electrolysis test in the wastewater are shown in Table 3. The results show that the removal efficiencies of PO $_{4}^{3-}$ and NO $_{3}^{-}$ were 100 %, while the removal of NH $_{4}^{+}$ was \sim 30 %. Furthermore, the batch reactor was able to remove \sim 85 % of Cl $_{4}^{-}$ and \sim 59 % of SO $_{4}^{2-}$.

The XRD patterns of the electrochemically obtained precipitates on the anode showed characteristic diffraction peaks for mostly magnesium hydroxide (Mg(OH)₂), (Fig. S.9 (a), ESI), while the precipitate formed on the cathode showed characteristic diffraction peaks for calcium carbonate or calcite (Fig. S.9 (b), ESI). It should be noted that the precipitate collected from the anode surface also showed a $\sim 3\,\%$ similarity to struvite based on a XRD database comparison, and we conclude that phosphate-based precipitates were formed based on the phosphate removal reported in Table 3. Phosphate precipitates can include struvite and magnesium phosphate. It is expected that the overall precipitate formed would be composed from a mixture of precipitates with multiple components, rather than one single component e.g., struvite, due to the complex nature of the real wastewater.

Previous studies performed by our group, where we investigated electrochemical struvite precipitation in synthetic wastewater showed that the crystallization followed a complex mechanism, where various (electro)chemical reactions occur simultaneously [39]. Studies using real wastewater demonstrated that while the chemical structure and morphology of the precipitate depends on the wastewater composition, high purity struvite can be produced by using appropriate pretreatment [40]. Precipitation and purity of struvite is mainly dependent on the pH with a high struvite content usually obtained at neutral to weakly basic pH (7.0-9.0), while above pH 9.5, the purity of struvite is expected to decrease sharply. The formation of primarily Mg(OH)2 on the anode (Fig. S.8, ESI) can be explained by the high pH measured in the bulk solution, which was ~ 11 . Moreover, it is expected that the local pH at the surface of the electrode would be 1.5-2.0 units higher, as elegantly shown by Moussa et al. [41] Overall, these results suggest that further optimization of the electrochemical reactor operating conditions (e.g., pH control) would improve struvite purity, but that an electrochemical precipitation approach holds promise for phosphate removal. Another possible approach to address the struvite precipitate quality is to pretreat and fractionate wastewater into multiple streams to separate nutrients at early stages using a multi-stage membrane system to avoid uncontrolled fouling during the preconcentration, enabling a high efficiency nutrient recovery from wastewater sources.

4. Conclusion

This study was performed to provide an initial framework for the selection of membranes for a multi-step membrane-based nutrient recovery system. The suggested multistage membrane design pursues optimization of nutrient capture from wastewater through three design goals: 1) nutrient pre-concentration, 2) phosphorus removal at early treatment stages, and 3) production of highly concentrated nitrogen stream as liquid organic fertilizer. Membranes were evaluated and selected for each goal based on the nutrient rejection performance. Polyamide TFC membranes with a highly charged and thin active layer were mostly effective in ammonium nutrient pre-concertation and can be used for down-stream struvite or direct liquid nitrogen fertilizer recovery. However, fully aromatic polyamide TFC resulted in a higher flux decline in high dissolved carbon wastewater; therefore, these

membranes had a lower preconcentration efficiency. The Alfa membrane, with large pore size, showed a high flux and very low flux decline in phosphorus concentration. This membrane is suggested for removal and preconcentration of phosphorus from wastewater streams at early stages, to recover P as struvite in down-stream and to prevent unwanted phosphorus precipitation in treatment plant equipment.

LCA was performed to analyze the environmental impact contribution of each configuration and to evaluate the sustainability of membrane-based preconcentration of nutrients for subsequent electrochemical struvite precipitation. LCA of preconcentration of nutrients with various configurations showed that increasing the number of membranes used in treatment of wastewater results in higher impacts from electricity required for pumping. These increased impacts can be partially offset by co-production of fertilizer. However, addition of membranes should be carefully considered depending on influent characterization and overall nutrient recovery that can be achieved. In addition, a combined membrane preconcentration of raw municipal wastewater and electrochemical nutrient precipitation was demonstrated. Although optimal fertilizer structure and preconcentration of raw wastewater is not achieved in this work, the combined testing showed that a complete phosphorus removal from raw municipal wastewater is obtained. This result showed the importance of a pretreatment step prior to nutrient preconcentration to eliminate suspended solids accumulation in the down-stream electrochemical reactor and highlighted the need for further investigation of the combined nutrient preconcentration-electrochemical precipitation in different wastewater sources.

CRediT authorship contribution statement

Zahra Anari: Methodology, Validation, Formal analysis, Investigation, Writing – original draft, Visualization. Karla Morrissey: Methodology, Validation, Formal analysis, Investigation, Writing – original draft, Visualization. László Kékedy-Nagy: Formal analysis, Investigation. Raheleh Daneshpour: Investigation, Visualization. Mojtaba Abolhassani: Investigation, Visualization. John Moore: Investigation. Greg Thoma: Conceptualization, Methodology, Writing – review & editing, Supervision, Project administration, Funding acquisition. Lauren Greenlee: Conceptualization, Methodology, Resources, Writing – review & editing, Supervision, Project administration, Funding acquisition.

Declaration of Competing Interest

The authors declare that they have no known competing financial interests or personal relationships that could have appeared to influence the work reported in this paper.

Data availability

Data will be made available on request.

Acknowledgements

LFG, ZA, and GT acknowledge funding support from the NSF I/UCRC MAST center, award # 1361809. KM acknowledges funding support from the National Science Foundation Graduate Research Fellowship program. LKN, LFG, and GT acknowledge funding support from the National Science Foundation through award # 1739473. The authors acknowledge support from the Arkansas Water Resources Center for analytical chemistry analysis of wastewater samples and the Institute of Nanoscience and Nanotechnology characterization facility at the University of Arkansas for support in surface and material characterization. The authors acknowledge mentorship, guidance, and advice from John Askegaard of Tyson Foods and Michael Watts of Garver, Inc. throughout the research performed for this paper. Finally, the authors thank the

Noland Wastewater Treatment Plant (Fayetteville, AR) for providing raw wastewater samples for testing as part of this study.

Appendix A. Supplementary data

Supplementary data to this article can be found online at https://doi.org/10.1016/j.seppur.2022.122907.

References

- J. Foley, D. de Haas, K. Hartley, P. Lant, Comprehensive life cycle inventories of alternative wastewater treatment systems, Water Res. 44 (5) (2010) 1654–1666.
- [2] P. Ledezma, P. Kuntke, C.J. Buisman, J. Keller, S. Freguia, Source-separated urine opens golden opportunities for microbial electrochemical technologies, Trends Biotechnol. 33 (4) (2015) 214–220.
- [3] Mohajit, K.K. Bhattarai, E.P. Taiganides, B.C. Yap, Struvite deposits in pipes and aerators, Biol. Wastes 30 (2) (1989) 133–147.
- [4] P.J. Talboys, J. Heppell, T. Roose, J.R. Healey, D.L. Jones, P.J.A. Withers, Struvite: a slow-release fertiliser for sustainable phosphorus management? Plant and Soil 401 (2016) 109–123.
- [5] L.E. de-Bashan, Y. Bashan, Recent advances in removing phosphorus from wastewater and its future use as fertilizer (1997–2003), Water Res. 38 (19) (2004) 4222–4246.
- [6] L. Kekedy-Nagy, J.P. Moore, M. Abolhassani, F. Attarzadeh, J.A. Hestekin, L. F. Greenlee, The passivating layer influence on Mg-based anode corrosion and implications for electrochemical struvite precipitation, J. Electrochem. Soc. 166 (12) (2019) E358–E364.
- [7] S. Ghosh, S. Lobanov, V.K. Lo, An overview of technologies to recover phosphorus as struvite from wastewater: advantages and shortcomings, Environ. Sci. Pollut. Res. 26 (19) (2019) 19063–19077.
- [8] H. Sun, A.N. Mohammed, Y. Liu, Phosphorus recovery from source-diverted blackwater through struvite precipitation, Sci. Total Environ. 743 (2020), 140747.
- [9] S. Hube, M. Eskafi, K.F. Hrafnkelsdóttir, B. Bjarnadóttir, M.Á. Bjarnadóttir, S. Axelsdóttir, B. Wu, Direct membrane filtration for wastewater treatment and resource recovery: A review. 710 (2020) 136375.
- [10] B. Al-Najar, C.D. Peters, H. Albuflasa, N.P. Hankins, Pressure and osmotically driven membrane processes: A review of the benefits and production of nanoenhanced membranes for desalination, Desalination 479 (2020), 114323.
- [11] G. Adam, A. Mottet, S. Lemaigre, B. Tsachidou, E. Trouvé, P. Delfosse, Fractionation of anaerobic digestates by dynamic nanofiltration and reverse osmosis: An industrial pilot case evaluation for nutrient recovery. 6 (2018) 6723-6732.
- [12] B.I. Escher, W. Pronk, M.J.F. Suter, M. Maurer, Monitoring the removal efficiency of pharmaceuticals and hormones in different treatment processes of sourceseparated urine with bioassays, Environ. Sci. Tech. 40 (16) (2006) 5095–5101.
- [13] N. Diaz-Elsayed, N. Rezaei, T.J. Guo, S. Mohebbi, Q. Zhang, Wastewater-based resource recovery technologies across scale: A review, Resour. Conserv. Recycl. 145 (2019) 94–112.
- [14] W. Pronk, H. Palmquist, M. Biebow, M. Boller, Nanofiltration for the separation of pharmaceuticals from nutrients in source-separated urine 40 (2006) 1405-1412.
- [15] C. Niewersch, A.L. Battaglia Bloch, S. Yüce, T. Melin, M. Wessling, Nanofiltration for the recovery of phosphorus - Development of a mass transport model 346 (2014) 70-78.
- [16] C. Blöcher, C. Niewersch, T. Melin, Phosphorus recovery from sewage sludge with a hybrid process of low pressure wet oxidation and nanofiltration 46 (2012) 2009-2019.
- [17] C. Wang, G.K. Such, A. Widjaya, H. Lomas, G. Stevens, F. Caruso, S.E. Kentish, Click poly(ethylene glycol) multilayers on RO membranes: Fouling reduction and membrane characterization. J. Membr. Sci. 409–410 (2012) 9–15.
- [18] K. Lee, Dissolved Organic Fouling on Nanofiltration Membranes, University of Alberta, Edmonton, Alberta, 2018.
- [19] R. Nitzsche, J. Köchermann, A. Gröngröft, M. Kraume, Nanofiltration of Organosolv Hemicellulose Hydrolyzate: Influence of Hydrothermal Pretreatment and Membrane Characteristics on Filtration Performance and Fouling, Ind. Eng. Chem. Res. 60 (2) (2021) 916–930.
- [20] A. Aziz, F. Basheer, A. Sengar, Irfanullah, S.U. Khan, I.H. Farooqi, Biological wastewater treatment (anaerobic-aerobic) technologies for safe discharge of treated slaughterhouse and meat processing wastewater, Sci. Total Environ. 686 (2019) 681–708.
- [21] J. Park, H.-F. Jin, B.-R. Lim, K.-Y. Park, K. Lee, Ammonia removal from anaerobic digestion effluent of livestock waste using green alga Scenedesmus sp, Bioresour. Technol. 101 (22) (2010) 8649–8657.
- [22] S. Du, D. Yu, J. Zhao, X. Wang, C. Bi, J. Zhen, M. Yuan, Achieving deep-level nutrient removal via combined denitrifying phosphorus removal and simultaneous partial nitrification-endogenous denitrification process in a single-sludge sequencing batch reactor, Bioresour. Technol. 289 (2019), 121690.
- [23] D8083-16, A., Standard Test Method for Total Nitrogen, and Total Kjeldahl Nitrogen (TKN) by Calculation, in Water by High Temperature Catalytic Combustion and Chemiluminescence Detection, 2016.
- [24] G. Wernet, C. Bauer, B. Steubing, J. Reinhard, E. Moreno-Ruiz, B. Weidema, The ecoinvent database version 3 (part I): overview and methodology. 21 (2016) 1218-1230.

- [25] C.I. Mendis, A. Singh, Magnesium Recycling: To the Grave and Beyond, JOM 65 (10) (2013) 1283–1284.
- [26] S. Ehrenberger, Update of Life Cycle Assessment of Magnesium Components in Vehicle Construction 2020.
- [27] L. Kékedy-Nagy, M. Abolhassani, R. Sultana, Z. Anari, K.R. Brye, B.G. Pollet, L. F. Greenlee, The effect of anode degradation on energy demand and production efficiency of electrochemically precipitated struvite, J. Appl. Electrochem. 52 (2) (2022) 205–215.
- [28] A. Ben-David, S. Bason, J. Jopp, Y. Oren, V. Freger, Partitioning of organic solutes between water and polyamide layer of RO and NF membranes: Correlation to rejection, J. Membr. Sci. 281 (1) (2006) 480–490.
- [29] S.-J. Kim, S. Kook, B.E. O'Rourke, J. Lee, M. Hwang, Y. Kobayashi, R. Suzuki, I. S. Kim, Characterization of pore size distribution (PSD) in cellulose triacetate (CTA) and polyamide (PA) thin active layers by positron annihilation lifetime spectroscopy (PALS) and fractional rejection (FR) method, J. Membr. Sci. 527 (2017) 143–151.
- [30] M. Cha, C. Boo, C. Park, Simultaneous retention of organic and inorganic contaminants by a ceramic nanofiltration membrane for the treatment of semiconductor wastewater, Process Saf. Environ. Prot. 159 (2022) 525–533.
- [31] P.-Y. Pontalier, A. Ismail, M. Ghoul, Mechanisms for the selective rejection of solutes in nanofiltration membranes, Sep. Purif. Technol. 12 (2) (1997) 175–181.
- [32] Y. Gu, Y.-N. Wang, J. Wei, C.Y. Tang, Organic fouling of thin-film composite polyamide and cellulose triacetate forward osmosis membranes by oppositely charged macromolecules, Water Res. 47 (5) (2013) 1867–1874.
- [33] P. Xu, J.E. Drewes, T.-U. Kim, C. Bellona, G. Amy, Effect of membrane fouling on transport of organic contaminants in NF/RO membrane applications, J. Membr. Sci. 279 (1) (2006) 165–175.

- [34] J. Luo, Y. Wan, Effects of pH and salt on nanofiltration—a critical review, J. Membr. Sci. 438 (2013) 18–28.
- [35] C.Y. Tang, Y.-N. Kwon, J.O. Leckie, Effect of membrane chemistry and coating layer on physiochemical properties of thin film composite polyamide RO and NF membranes: I. FTIR and XPS characterization of polyamide and coating layer chemistry 242 (2009) 149-167.
- [36] E.M. Vrijenhoek, S. Hong, M. Elimelech, Influence of membrane surface properties on initial rate of colloidal fouling of reverse osmosis and nanofiltration membranes, J. Membr. Sci. 188 (1) (2001) 115–128.
- [37] C. Kappel, An Integrated Membrane Bioreactor-Nanofiltration Concent with Concentrate Recircultation for Wastewater Treatment and Nutrient Recvoery, Universiteit Twente (2014).
- [38] S.P. Chesters, Innovations in the inhibition and cleaning of reverse osmosis membrane scaling and fouling, Desalination 238 (1) (2009) 22–29.
- [39] L. Kekedy-Nagy, A. Teymouri, A.M. Herring, L.F. Greenlee, Electrochemical removal and recovery of phosphorus as struvite in an acidic environment using pure magnesium vs. the AZ31 magnesium alloy as the anode, Chem. Eng. J. 380 (2020) 7
- [40] L. Kékedy-Nagy, M. Abolhassani, S.I. Perez Bakovic, Z. Anari, J.P. Moore Ii, B. G. Pollet, L.F. Greenlee, Electroless Production of Fertilizer (Struvite) and Hydrogen from Synthetic Agricultural Wastewaters, J. Am. Chem. Soc. 142 (44) (2020) 18844–18858.
- [41] S. Ben Moussa, G. Maurin, C. Gabrielli, M. Ben Amor, Electrochemical precipitation of struvite, Electrochem. Solid State Lett. 9 (6) (2006) C97–C101.